Communication

Single Molecule Charging by Atomic Force Microscopy

Chuleekorn Chotsuwan, and Silas C. Blackstock

J. Am. Chem. Soc., **2008**, 130 (38), 12556-12557 • DOI: 10.1021/ja802419y • Publication Date (Web): 30 August 2008

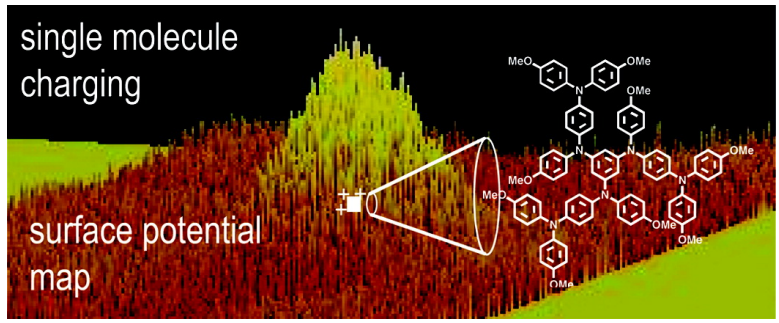

More About This Article

Additional resources and features associated with this article are available within the HTML version:

- Supporting Information
- Access to high resolution figures
- Links to articles and content related to this article
- Copyright permission to reproduce figures and/or text from this article

View the Full Text HTML

J|A|C|S
COMMUNICATIONS

Published on Web 08/30/2008

Single Molecule Charging by Atomic Force Microscopy

Chuleekorn Chotsuwan and Silas C. Blackstock*

Department of Chemistry and The Center for Materials for Information Technology, The University of Alabama, Tuscaloosa, Alabama 35487

Received April 2, 2008; E-mail: blackstock@ua.edu

The positioning of discrete molecular charges in solids with nanometer resolution can enable high-resolution information storage,[1] electrostatic patterning,[2] and gating of molecular conductivity.[3] In previous work, we reported on hole injection into neat molecular films composed of specially structured polyarylamines.[4] We now report AFM charging of arylamines embedded in polymethylmethacrylate (PMMA) films and demonstrate *the charging of single molecules* in these films.

The ability to monitor redox events of just a few or even single molecules is an exciting new development made possible by the recent emergence of single molecule detection techniques.[5] Some time ago, Gemma et al. reported charge injection by AFM into 30−50 nm arylamine islands on SiO_2.[6] More recently, charge switching of a single copper phthalocyanine molecule by STM at a double barrier tunnel junction was reported.[7] In this work, both charge switching and detection are achieved by ambient AFM on small domains of polyarylamines, down to the single molecule limit.

The charge carriers of this study are oligoarylamines (known generally as hole transport agents[8]) **1**, a prototype redox-gradient dendrimer developed for charge storage applications (i.e., low conductivity),[9] and **2**, a tris(*p*-phenylene-diamine), also developed in our laboratory.[10] Both substrates afford thermally stable isolable polycations. The oxidation potentials measured by cyclic voltammetry in CH_2Cl_2 (0.1 M Bu_4NBF_4) are 0.72, 1.08, and 1.62 V for **1** and 0.45, 0.59, 0.65, 1.00, 1.06, and 1.12 V vs SCE for **2**.

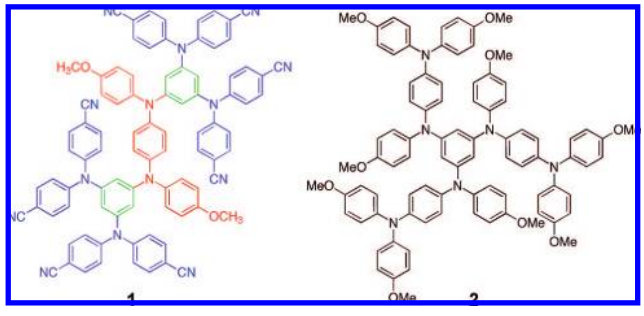

Thin films (3.0 nm, by ellipsometry) of polyamines **1** and **2** in PMMA were spin coated on silicon substrates containing a 25 nm SiO_2 layer. Tapping AFM shows molecularly smooth films (R_{rms} = 0.17−0.18 nm). Application of a +6 V tip bias in tapping mode with a reduced set point selectively charges the amine (charge carrier) and not the polymer (Figure 1), as detected by Kelvin probe microscopy[11] (KPM).

For both **1**/PMMA and **2**/PMMA films, the observed peak potential after charging scales with the carrier concentration in the film (see Figure 2 for **1**/PMMA). Also, the threshold voltage needed to charge the amines scales with their respective solution oxidation potentials (i.e., V_{th} = 4 V for **1** and 1 V for **2**). At high dilution (≤2 wt%) the charging of either the **1** or **2** film generates a constant surface potential value, suggesting a minimum charge state.

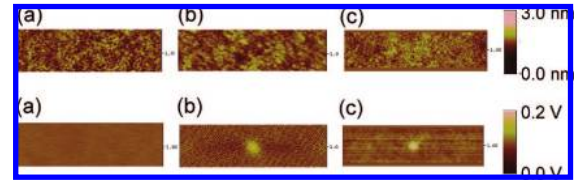

Figure 1. Film morphology (top) and surface potential (bottom) after applied tip bias of 6 V for (a) neat PMMA, (b) 10 wt% **1**/PMMA, and (c) 10 wt% **2**/PMMA. Images are 2 μm × 0.5 μm.

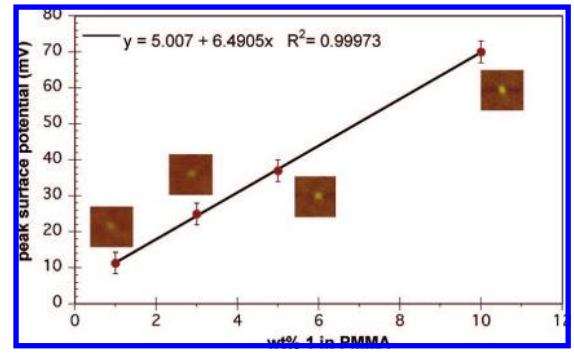

Figure 2. KPM peak surface potential of AFM-charged domain as a function of wt% **1** in 3 nm PMMA films on SiO_2/Si. Insets are 1 × 1 μm^2 KPM potential maps.

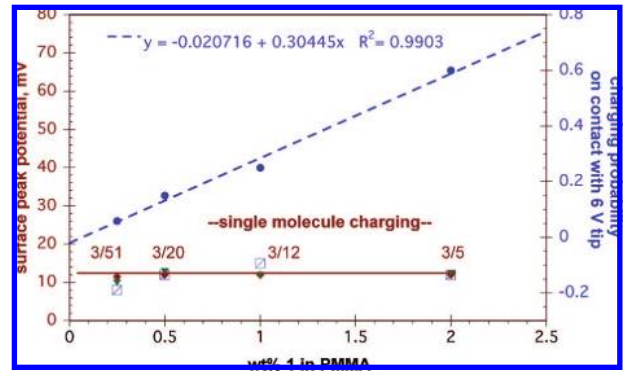

Figure 3. (Red) Peak surface potential (with charge per attempt ratio given for each film) measured after probe charging with 6 V tip bias and (blue) probability of charging the dilute **1**/PMMA 3 nm films upon contact with 6 V tip.

Moreover, the films become statistically more difficult to charge (i.e., not every attempt results in film charging) as the amine content decreases (see Figure 3). The plateau potential and linear charging statistics indicate *single molecule charging* of arylamines in homogeneous PMMA films.

From Figure 3 data we may extract an effective tip charging radius for AFM charging under these conditions. Equating the densities of **1** and PMMA[12] at 1.2 g/cm^3 yields an effective packing

10.1021/ja802419y CCC: $40.75

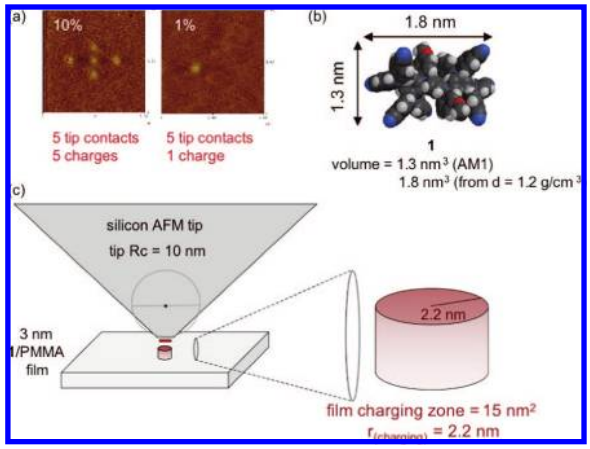

Figure 4. (a) Representative KPM maps of five charging attempts in 10 and 1.0 wt% **1**/PMMA 3 nm films on SiO_2/Si, (b) AM1 footprint of **1**, and (c) estimated AFM-charging metrics.

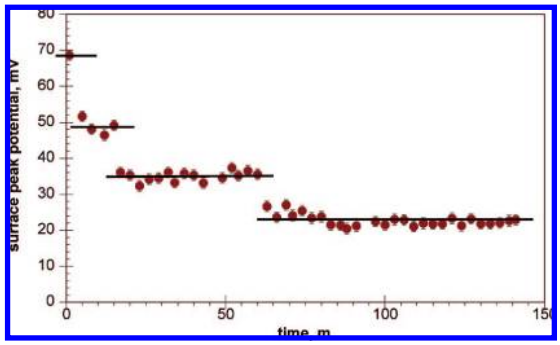

Figure 5. Surface potential decay of individually charged **2** in 3 nm PMMA film.

volume of 1.83 nm^3 for a single molecule of **1** and an average 183 nm^3 volume per molecule in a 1.0 wt% **1**/PMMA film. The charging statistics correspond to 0.25 molecule per tip charging event, yielding an effective tip charging volume of 46 nm^3. If we approximate the charging zone as a cylinder of 3.0 nm height (the film thickness), then the tip charging surface area must be ~15 nm^2 and the effective tip charging radius (r_{char}) is ~2.2 nm for the commercial silicon r_{curv} = 10 nm tips used in this experiment (confirmed by SEM measurement). These results are summarized in Figure 4.[13]

Even for the single molecular charge, the KPM surface potential map half-width is ~100 nm, roughly 75× the charge size. KPM is known to overestimate feature sizes,[14] in part because of the distance dependence of the electric field force and because the applied potential to the tip/cantilever represents, in this case, a much larger charge volume than the film charge and so the former dominates the potential map.

The temporal KPM analysis of a single molecular ion shows discontinuities as shown for a single charge carrier **2** formed by AFM charging (8 V tip bias) of a 1 wt% **2**/PMMA film (Figure 5). This polyamine can attain +1 to +6 states in solution.[10] The steps in the surface potential appear to be quantized charge state changes for the single molecule as it discharges. If the initial 70 mV peak potential corresponds to $\mathbf{2}^{6+}$, then we can tentatively assign the 11 mV steps in the discharge profile to elementary charge transitions for **2**.

The detailed mechanisms of charging and charge decay are under further study. It is observed that the surface potential decay rate for **2** cations decreases as the substrate SiO_2 layer thickness is increased, suggesting reduction of the molecular charge by electrons from the silicon. These measurements are made under ambient conditions, so charge passivation from the environment may also play a role in surface potential decay. The polyamine can be recharged after "neutralization" and a similar stepped discharge is again observed, indicating that the process is reversible.

In summary, we have demonstrated selective charging of polyamines **1** and **2** embedded in a PMMA matrix. Under ambient conditions, the charging and direct observation of a single charged molecule has been accomplished. The metric resolution of the AFM charging process and KPM surface potential mapping has been established for these experiments. Quantized discharge of single, multicharged polyamines is observed. These findings allow charge switching of individual redox molecules and subsequent direct study of single ions in varied environments relevant to molecular function in devices.

Acknowledgment. We thank the National Science Foundation for support of this research (CHE-0079272 and DMR-00213985) and the Thailand Institute for the Promotion of Teaching Science and Technology for a tuition scholarship to C.C.

Supporting Information Available: Experimental details of substrate and film preparations, film thickness measurements, AFM/KPM instrumentation and data collection parameters, SEM of AFM tip, voltage profiles for AFM charging of 10 wt% **1** and **2** in PMMA, and SiO_2 thickness dependence of surface potential decay. This information is available free of charge via the Internet at http://pubs.acs.org/.

References

(1) (a) Liu, Z.; Yasseri, A. A.; Lindsay, J. S.; Bocain, D. F. *Science* **2003**, *302*, 1543–1545. (b) Liu, C.-Y.; Bard, A. J. *Acc. Chem. Res.* **1999**, *32*, 235–245. (c) Green, J. E.; Choi, J. W.; Boukai, A.; Bunimovich, Y.; Johnston-Halperin, E.; DeIonno, E.; Luo, Y.; Sheriff, B. A.; Xu, K.; Shin, Y. S.; Tseng, H.-R.; Stoddart, J. F.; Heath, J. R. *Nature* **2007**, *445*, 414–417.

(2) (a) Seemann, L.; Stemmer, A.; Naujoks, N. *Nano Lett.* **2007**, *7*, 3007–3012. (b) Ressier, L.; Le Nader, V. *Nanotechnology* **2008**, *19*, 135301–135307.

(3) (a) Xiao, X.; Brune, D.; He, J.; Lindsay, S.; Gorman, C. B.; Tao, N. *Chem. Phys.* **2006**, *326*, 138–143. (b) Kanwal, A.; Chhowalla, M. *Appl. Phys. Lett.* **2006**, *89*, 203103. (c) Kushmerick, J. G.; Blum, A. S.; Long, D. P. *Anal. Chim. Acta* **2006**, *568*, 20–27.

(4) (a) Li, J. C.; Blackstock, S. C.; Szulczewski, G. J. *J. Phys. Chem. B* **2006**, *110*, 17493–17497. (b) Li, J. C.; Kim, K.-Y.; Blackstock, S. C.; Szulczewski, G. J. *Chem. Mater.* **2004**, *16*, 4711–4714.

(5) (a) For single molecule detection by scanning electrochemical microscopy in solution, see: Fan, F. R.; Bard, A. J. *Science* **1995**, *268*, 1883. (b) For single polymer particle spectroelectrochemistry, see: Palacios, R. E.; Fan, F.-R. F.; Grey, J. K.; Suk, J.; Bard, A. J.; Barbara, P. F. *Nat. Mater.* **2007**, *6*, 680–685. (c) For STM analysis of absorbed porphyrin molecules at an electrode surface, see: He, Y.; Borguet, E. *Angew. Chem., Int. Ed.* **2007**, *46*, 6098–6101.

(6) Gemma, N.; Hieda, H.; Tanaka, K.; Egusa, S. *Jpn. J. Appl. Phys.* **1995**, *34*, L859–L862.

(7) Mikaelian, G; Ogawa, N.; Tu, X. W.; Ho, W. *J. Chem. Phys.* **2006**, *124*, 131101.

(8) Shirota, Y.; Kageyama, H. *Chem. Rev.* **2007**, *107*, 953–1010.

(9) RGD **1** synthesis and electrochemistry: Duncan, J. R. Changing the Redox-Gradient in Geometrically Equivalent Aryl Amine, Ph.D. Dissertation, The University of Alabama, 2007.

(10) Stickley, K. R.; Selby, T. D.; Blackstock, S. C. *J. Org. Chem.* **1997**, *62*, 44.

(11) For a review, see: Palermo, V.; Palma, M. *Adv. Mater.* **2006**, *18*, 145–164.

(12) The density for ~15 000 M_w PMMA (Aldrich) is 1.2 g/mL. The density of *N*,*N*,*N*′,*N*′-tetra(*p*-anisyl)-*p*-phenylenediamine from its X-ray crystal structure of 1.233 g/mL (173 K) is used here as a model for the density of **1** and **2**.

(13) If the charging depth is less than 3 nm, then the estimated r_{char} will increase. For a charging zone of a cylinder of 1 nm depth, r_{char} becomes 3.8 nm. Further experiments are underway to pinpoint this value.

(14) (a) Kalinin, S. V.; Bonnell, D. A.; Freitag, M.; Johnson, A. T. *Appl. Phys. Lett.* **2002**, *81*, 754–756. (b) Lü, J.; Delamarche, E.; Eng, L.; Bennewitz, R.; Meyer, E.; Güntherodt, H.-J. *Langmuir* **1999**, *15*, 8184–8188.

JA802419Y